Electrical Power and Energy Systems 141 (2022) 108254

Contents lists available at ScienceDirect

International Journal of Electrical Power and Energy Systems

journal homepage: www.elsevier.com/locate/ijepes

Modified Complete Ensemble Empirical Mode Decomposition based HIF detection approach for microgrid system

Monalisa Biswal [a], Ch. Durga Prasad [a], Papia Ray [b], Nand Kishor [c,*]

[a] Department of Electrical Engineering, National Institute of Technology Raipur, 492010, Chhattisgarh, INDIA
[b] Department of Electrical Engineering, Veer Surendra Sai University of Technology Burla, 768018, Odisha, INDIA
[c] Department of Engineering, Østfold University College, Fredrikstad campus, Norway

ARTICLE INFO

Keywords:
System unbalance
Grounding transformer
Distribution system
Islanding
Signal decomposition
Current signal

ABSTRACT

Detection of high impedance fault (HIF) in an active distribution system is a challenging task. It is learned from the fault characteristics that detection and discrimination of HIF during different critical conditions is impossible using the fault current magnitude. Under dependable situations such as energization of a transformer, nonlinear load and capacitor bank detection and discrimination of HIF is challenging. In a distribution system with an inverter based distributed generator (IBDG), the current contribution during islanding mode is very low and also for HIF condition. To mitigate these issues, an intelligent approach applying Modified Complete Ensemble Empirical Mode Decomposition with Adaptive Noise (MCEEMDAN) on residual current signal is developed. The second intrinsic mode function (IMF2) is extracted using MCEEMDAN and its Teager Kaiser Energy Operator (TKEO) is computed to detect and discriminate the HIF against other physical events. The novelty of MCEEMDAN approach lies with its noise free output and faster response as compared to other time–frequency approaches. The method is tested for several fault and non-fault cases including, presence of noise, harmonics, and unbalance loadings. The comparison with recently reported techniques for very HIF and ungrounded system proofs the efficacy of the method.

1. Introduction

Majority of the high impedance faults (HIFs) takes place in the distribution network of the voltage level below 25 kV [1]. The low-level current magnitude during such fault makes the condition undetectable by the conventional overcurrent relay. The HIF, because of the fault path, can be classified as a broken and unbroken type. In a broken type, the faulty conductor makes a contact with a poor conductive path such as sand, grass, asphalt, etc., where the signature of current does not introduce significant variation so as to be detected as a fault. In the present scenario, the passive distribution system is under transformation into active grid, so that sustainable growth in the power sector can be achieved. In this context, distributed generation (DG) resources such as wind turbines and photovoltaic are integrated at the distribution level. The use of power electronic inverters in the DG system undoubtedly improves the reliability, security of power supply and enhances the power efficiency. However, fault identification challenges in an inverter-based system cannot be avoided [1]. In the recent years, various methods have been proposed to detect HIF considering the operational impact of inverter system in the active distribution network and stochastic fault current signature [2–20].

HIF cannot be detected reliably using conventional approach and due to the downed conductor on the distribution side, the public risk factor increases [2]. This low current fault tends to exhibit nonlinear variations in signal, characterized by the presence of higher frequency components and harmonics [3]. So, many protection engineers and researchers exploit this current signal to develop secure protection functions. Details of the previous research work have been well documented [4–20].

Fast and reliable detection of HIF is essential, so that uninterrupted and quality power can be ensured to end users of the distribution side. To extract adequate features, different techniques based on Kalman Filtering [4], mathematical morphology [5,6], Hilbert-Transform [7], Finite Impulse Response (FIR) filters [8–10], wavelet transform [11–13], energy variance criterion [14] and fractal theorem [15] have been reported to detect HIF. Expert system [5,16] based heuristic approaches are also available in this context. The occurrence rate and severity of HIF is high in distribution system of voltage level below 15 kV, but for voltage level up to 25 kV, the severity level gradually reduces. So, the

* Corresponding author.
E-mail addresses: mbiswal.ele@nitrr.ac.in (M. Biswal), papia_ray@yahoo.co.in (P. Ray), nand_research@yahoo.co.in, nand.kishor@hiof.no (N. Kishor).

https://doi.org/10.1016/j.ijepes.2022.108254
Received 8 September 2021; Received in revised form 28 February 2022; Accepted 11 April 2022
Available online 20 April 2022

Nomenclature

k, m	Mode
W^i	White Gaussian Noise
E_k	Local mean
r_1	Residue
α	Signal to Noise Realization lies in the range 0 to 1
ε_m	Coefficient of variation
Ψ	Discrete TKEO
HIF	High Impedance Fault
DG	Distributed Generation
CC	Capacitor Charging
NLS	Nonlinear Load Switching
TS	Transformer Switching
VMD	Variational Mode Decomposition
TKEO	Teager Kaiser Energy Operator
IMF	Intrinsic Mode Function
CEEMDAN	Complete Ensemble Empirical Mode Decomposition with Adaptive Noise
MCEEMDAN	Modified CEEMDAN
EMD	Empirical Mode Decomposition
DFIG	Doubly Fed Induction Generator
WGN	White Gaussian Noise
SNR	Signal-to-Noise Ratio
PV	Photovoltaic

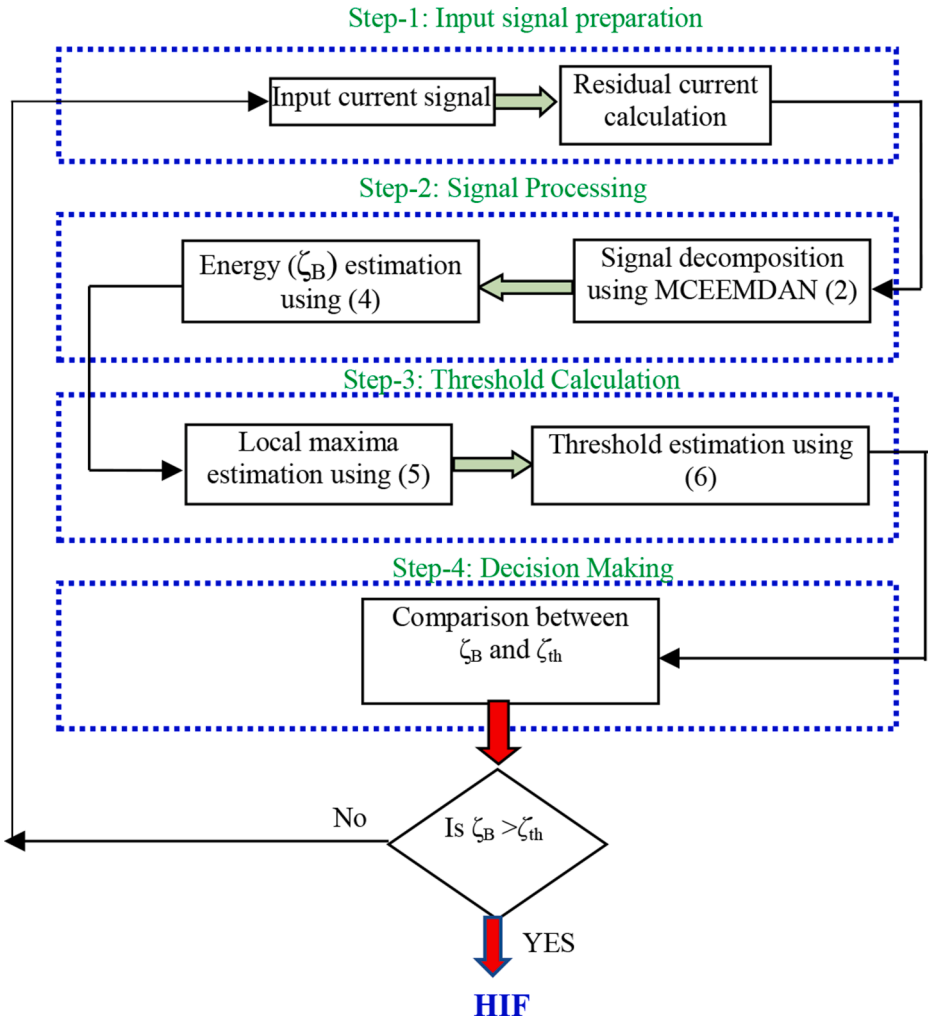

Fig. 1. Computational steps for the proposed method.

studies on HIF are restricted only to voltage level below 15 kV. The occurrence of HIFs is associated with arcing phenomenon and due to this, the current signal remains highly nonlinear. As a result, the existence of different order of frequency components is quite obvious, among which, higher order frequency component is more significant [1]. So, time–frequency analysis-based approaches have been applied by many researchers to mitigate against the detection challenges [11–13,17–21]. Although detection of HIF is challenging but at the same time, the detection algorithm should be able to discriminate other dependable events such as capacitor charging (CC), nonlinear load switching (NLS), transformer switching (TS) etc. In the line of above discussion, a Variational Mode Decomposition (VMD) based HIF detection technique is proposed in [18] to detect and discriminate HIF from other switching events.

Distribution system is unbalance in nature and the presence of noise and harmonics due to the switching of power electronics devices

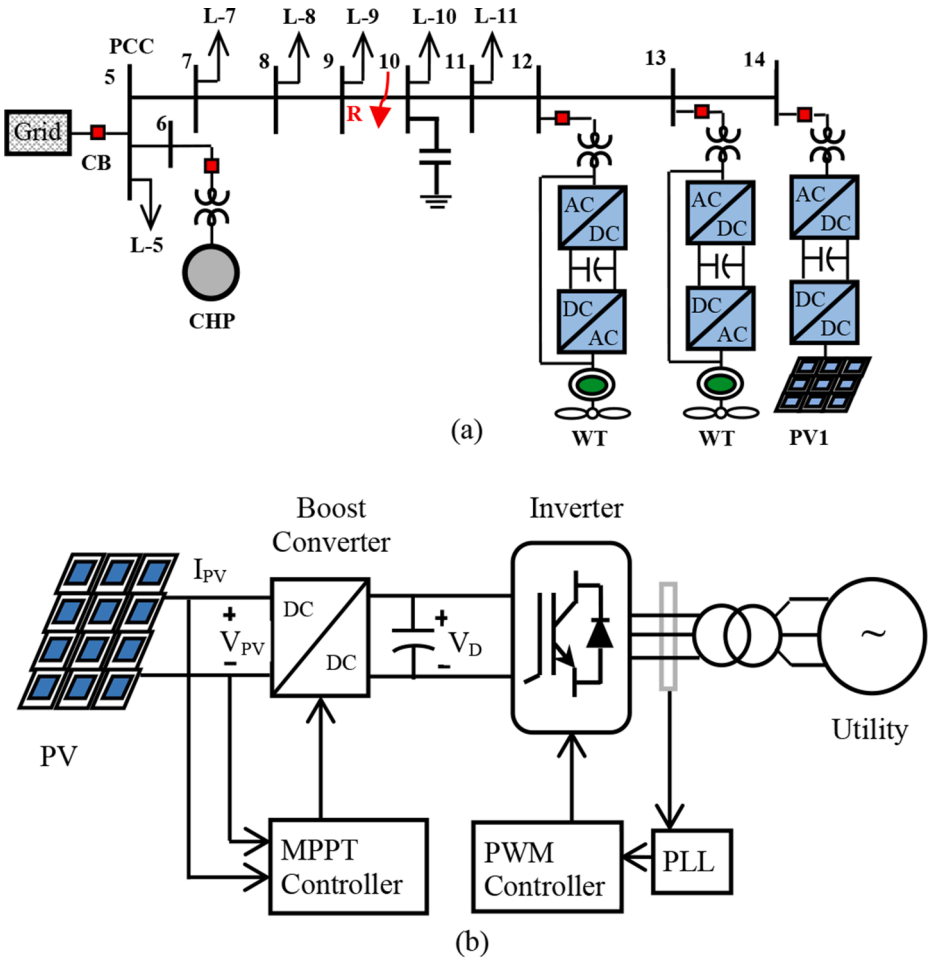

Fig. 2. (a) Structure of test system. (b) Grid-connected PV system.

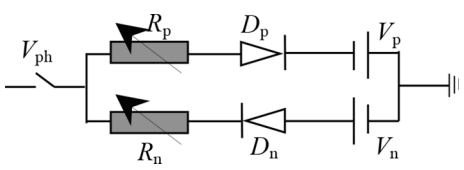

Fig. 3. HIF model.

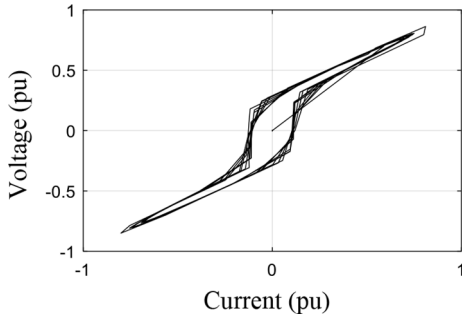

Fig. 4. V-I characteristic of HIF.

associated with renewable sources may further deteriorate the system generated signal. The main aspect of protection function is to take quick decision and that too securely, which surely needs a reliable enhanced protection algorithm.

In this work, a scheme based on MCEEMDAN (Modified Complete Ensemble Empirical Mode Decomposition with Adaptive Noise) approach is developed to detect HIF. Previously, MCEEMDAN has already been applied for many applications [22–24]. The proposed method in this paper offers several merits such as:

1. Adaptive selection of low pass filter which gives best result in the presence of noise.
2. Fast, secure, accurate and reliable
3. Robust for any configurated network

Here, the most effective mode i.e., second mode (IMF2) is extracted as discussed later. The energy of IMF2 is estimated to detect the HIF. Unlike other decomposition algorithms, buffered signal is passed through the processing algorithm so as to meet the relay requirement. The development stages of proposed method involves the computation of residual current calculation, signal decomposition using MCEEMDAN approach, TKEO computation for the suitable mode considering the recursive window. Also, the high frequency component mode is extracted. Adaptive threshold is applied to identify the fault event. The article is organized in the following manner. The proposed approach for fault detection is discussed in Section II. Distribution system architecture and fault characteristics are provided in Section III. Section IV validates the response of the proposed scheme and comparative report with other existing approaches. Finally, the conclusion is given in Section V.

2. HIF detection using novel MCEEMDAN and Teager-Kaiser energy operator

Except on rare occasion, the HIF is associated with an initiation of an

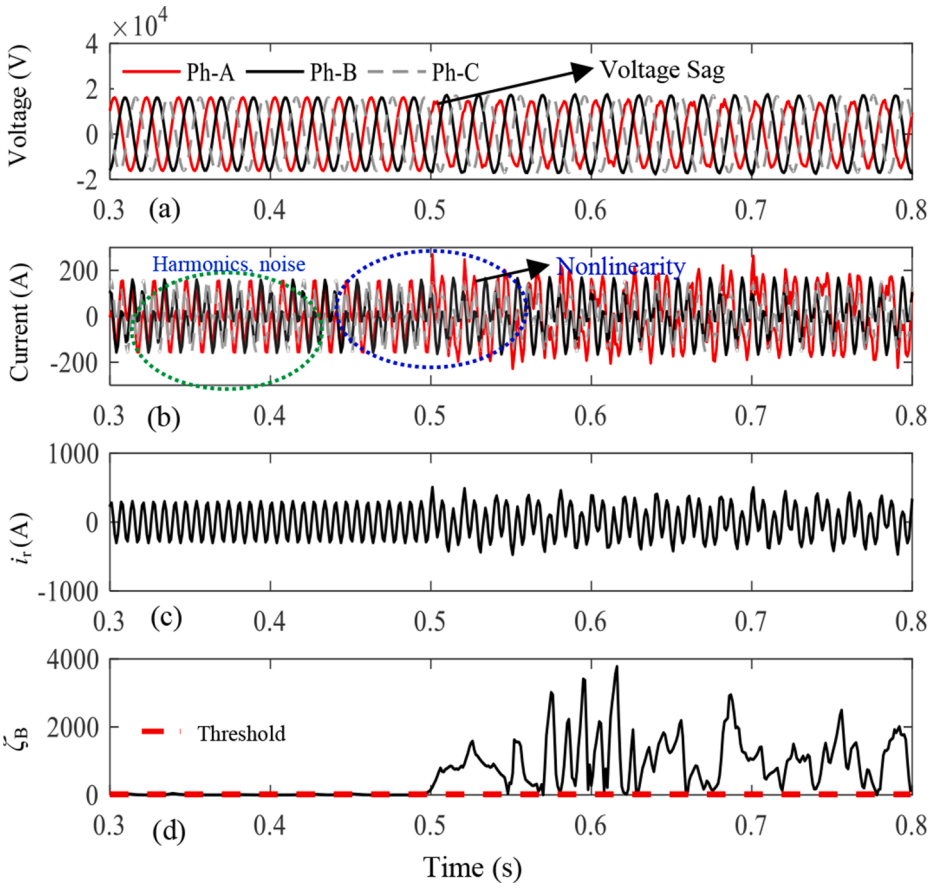

Fig. 5. Response for fault associated with voltage sag, noise, harmonics and unbalance.

Table 1
Simulated Cases for Different SNRs, Percentage Loading and Order of Harmonics.

Cases	SNR (dB)	Ph-A Loading (%)	Ph-B Loading (%)	Ph-C Loading (%)	Order of Harmonic
1	5	30	–	–	3rd, 5th
2		–	40	–	
3		–	–	45	
4	10	25	–	–	3rd, 5th
5		–	35	–	
6		–	–	50	
7	15	20	–	–	3rd, 5th
8		–	25	–	
9		–	–	30	
10	20	15	–	–	3rd, 5th
11		–	40	–	
12		–	–	50	
13	25	10	–	–	3rd, 5th
14		–	20	–	
15		–	–	30	
16	30	35	–	–	3rd, 5th
17		–	45	–	
18		–	–	50	

arcing phenomenon. The random pattern and small variations in current magnitude are highly dependent on the fault path and fault conditions [1]. The common features of HIF involve intermittence, asymmetry, nonlinearity, buildup, shoulder, randomness and long duration [12]. Due to this fact, conventional relay settings are unsuitable to identify the HIF, which allows the event to sustain for longer duration i.e., seconds to several hours. For the possible detection of HIF, the harmonics patterns such as 2nd, 3rd, and 5th of fault characteristics are analyzed in [25,26]. Using time–frequency based approaches, the signals can be analyzed and the effective features associated with HIF can be detected. In the system, generation of switching transient due to sudden activation of any circuit device or components can bring in further challenges. Such switching events can also involve the presence of even and odd harmonic components in the signal. So, protection function should be secure as well as dependable to handle all fault and non-fault conditions. It becomes important to distinguish and detect the faulty events against non-faulty events using more advanced signal processing technique. Considering the existing challenges and the basic requirement for protection relay, an adaptive and enhanced signal decomposition based approach, the HIF detection logic is developed in this study.

A Modified Complete Ensemble Empirical Mode Decomposition with Adaptive Noise (MCEEMDAN)

In this work, the MCEEMDAN approach is used to analyze the fault generated signal so as to extract the intermittence and randomness components. The EMD and EEMD suffers in accurate identification of different oscillatory modes present in the signal [27,28]. As a result, mode mixing problem arises. Due to this, an IMF falsely shows different physical processes represented in the mode. The CEEMDAN algorithm has certain drawbacks such as decomposition of the given signal into spurious modes and presence of residual noise in the decomposed modes [22]. To overcome this, the proposed modified CEEMDAN (MCEEMDAN) scheme has been developed.

The MCEEMDAN clearly identifies the oscillatory modes present in the non-linear and non-stationary signal. Both CEEMDAN and MCEEMDAN algorithms are same, except the noise removal capacity. The spurious modes and residual noise problems can be solved using MCEEMDAN technique. Using the said technique different intrinsic mode functions (IMFs) can be extracted and the most suitable one is used

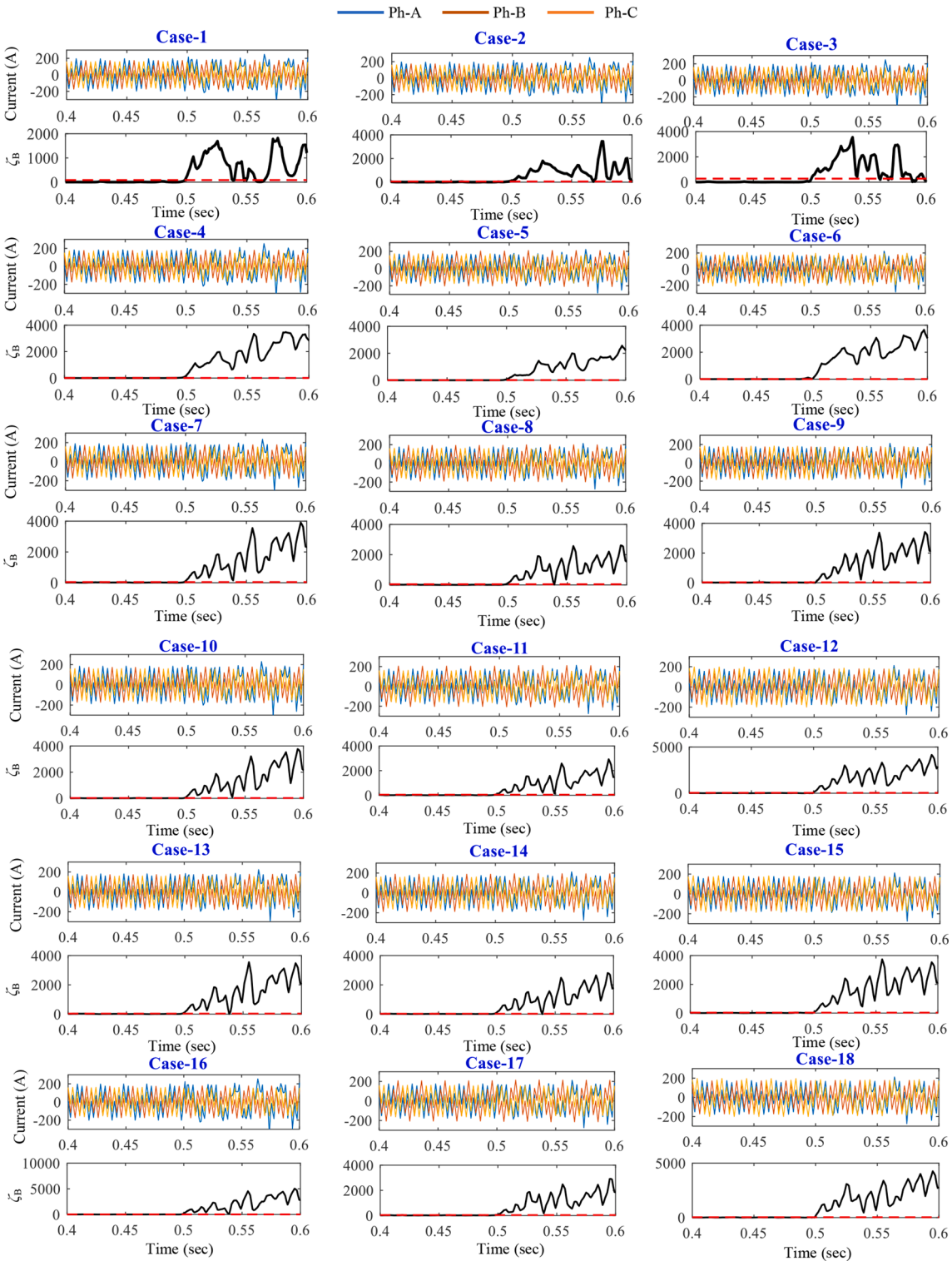

Fig. 6. Performance of detection algorithm for different SNR, percentage loading and with presence of harmonics.

for further analysis in obtaining fault index. The detailed MCEEMDAN algorithm is described below [22].

Let $LM(.)$ be the operator that gives signal's local mean, $E_k()$ operator represents the 'k^{th}' mode obtained by EMD and W^i be the white Gaussian noise with zero mean and unity variance. So, the steps executed are:

a) **Step-1.** Estimate the local mean of the signal–noise realization $S^i = S + \alpha_0 E_1(W^i)$ to acquire the first residue $r_1 = LM(S^i)$ by implementing EMD scheme.
b) **Step-2.** Obtain the first mode by $mode_1 = \mathrm{M}_1 = S - r_1$.
c) **Step-3.** Determine the second residue as the average of all the local mean of the realization,$r_1 + \alpha_1 E_2(W^i)$. where 'α' is signal to noise realization which is expressed as:

$$\alpha_m = \varepsilon_m \mathrm{std}(r_m) \tag{1}$$

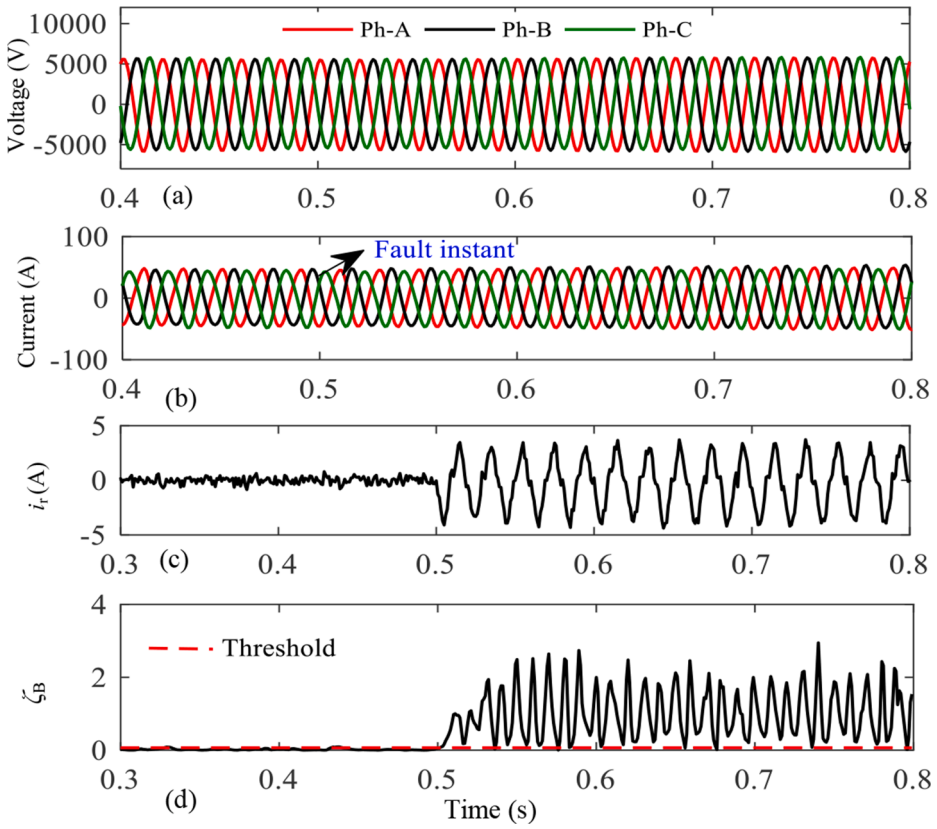

Fig. 7. Response during islanded mode of operation. SNR = 10 dB, *R*p and *R*n = 1 ~ 1.35 kΩ.

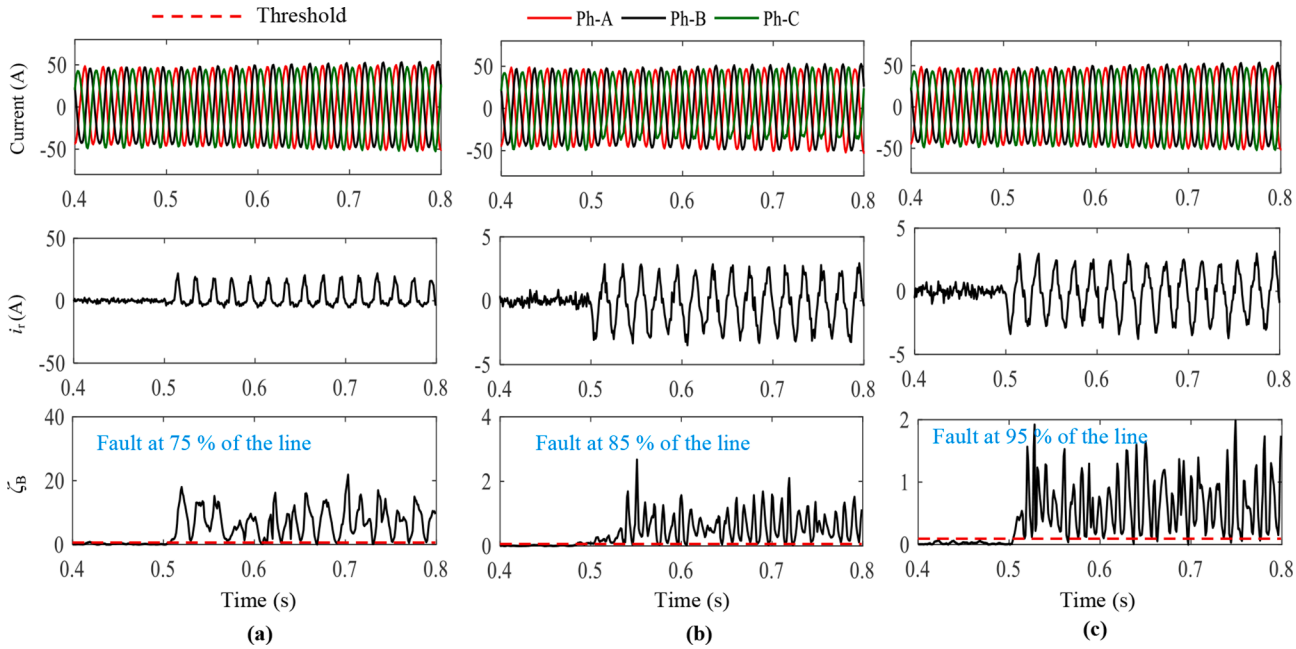

Fig. 8. Response of the method for fault at (a) 75 % of the line, (b) 85 % of the line and (c) 95 % of the line from relay location. SNR = 10 dB, *R*p and *R*n = 1.35 ~ 1.5 kΩ.

Here, ε_m represents coefficient of variation of the 'm^{th}' mode, 'std' denotes standard deviation and 'r_m' is the m^{th} residue.

d) **Step-4.** For $k = 3, 4, \ldots.K$, calculate the k^{th} residue

$$r_k = \langle LM(r_{k-1} + \alpha_{k-1}E_k(W^i))\rangle \quad (2)$$

e) **Step-5.** Estimate the k^{th} mode i.e., $\text{mode}_k = r_{k-1} - r_k$

f) **Step-6.** Go to step-4 for next k.

In order to get a constant SNR (α) instead of increasing one as in other masking based EMD schemes, α in (1) is to be set in such a way that

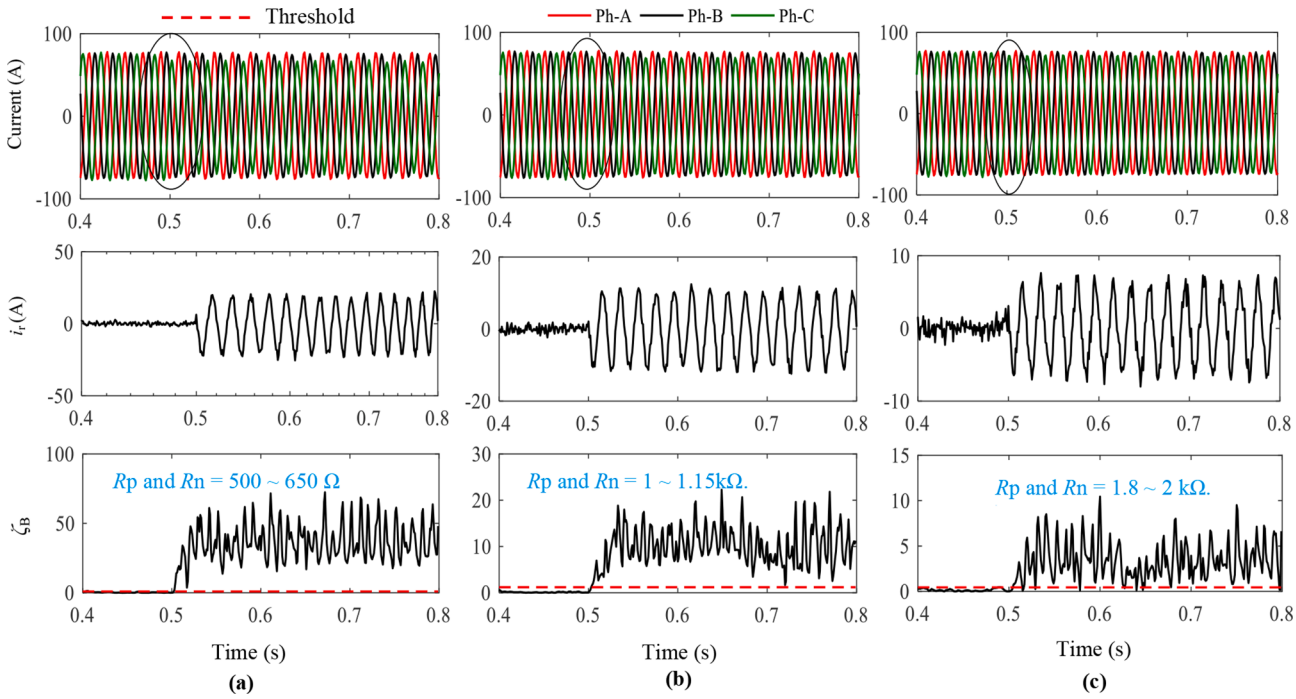

Fig. 9. Response of the method for different fault resistances in the range (a) 500 ~ 650 Ω, (b) 1 ~ 1.15 kΩ, (c) 1.8–2 kΩ. SNR = 5 dB, fault location = 85% of the line.

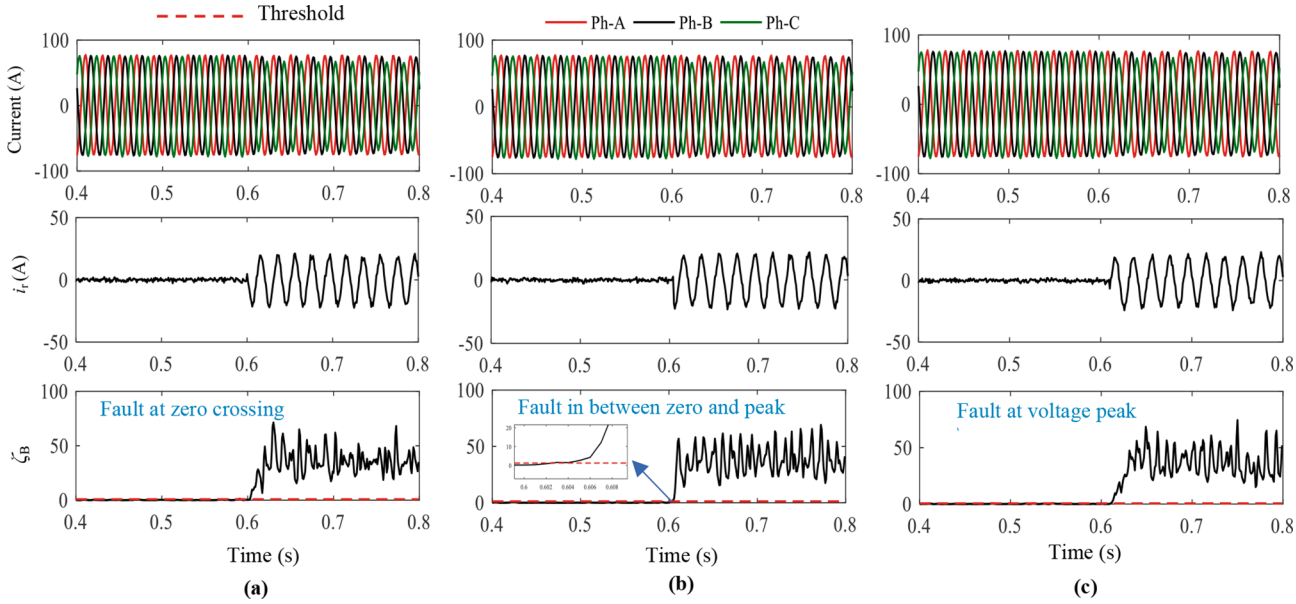

Fig. 10. Response of the method for different fault inception point on voltage wave. (a) Zero crossing, (b) In between zero and Peak point, (c) peak point on voltage wave. SNR = 5 dB, fault location = 85% of the line.

the coefficient of variation (ε) becomes exactly the reciprocal of the SNR of the initial added noise with the signal.

To make the developed algorithm suitable for common relaying platform, 1 kHz sampling rate is considered. As discussed earlier, the presence of even and odd harmonics is more prominent during HIF as per the earlier reported works. As discussed later, IMF2 is analyzed in this work to calculate the fault index. The HIFs are associated with evolution of large energy at the instant of fault inception and thus, its instant of occurrence can be estimated via calculation of the energy operator. Next section will give the various formulated steps to identify HIF using suitable IMF and energy operator.

B MCEEMDAN based Detection Principle

The residual current (i_r) can be computed at any instant using (3).

$$i_r(t) = i_a(t) + i_b(t) + i_c(t) \tag{3}$$

Then, i_r is processed through MCEEMDAN and the second IMF (M_2) can be estimated. M_2 is then used to estimate the TKEO (ζ_B) using (4).

$$\zeta_B = |\psi[M_2(n)]| = \left|M_2(t)^2 - M_2(t-1)M_2(t+1)\right| \tag{4}$$

where,Ψ is the discrete Teager energy operator. The Teager energy of different IMFs are estimated and from the obtained results, it is observed

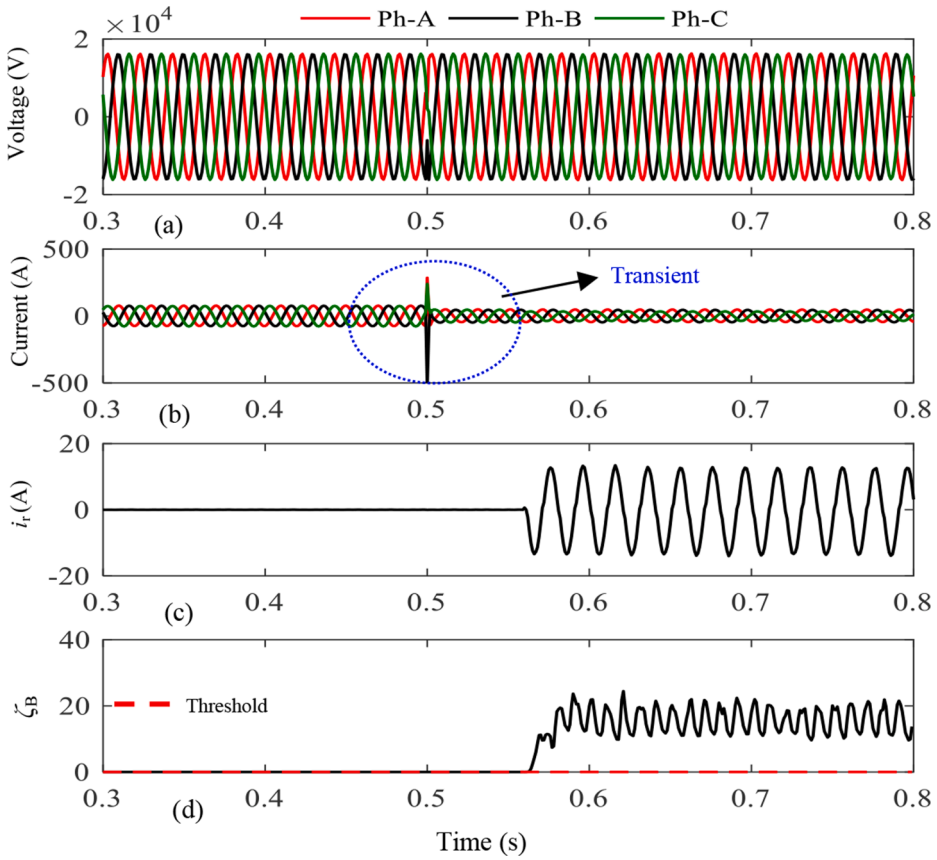

Fig. 11. Response for capacitor charging and HIF.

that the Teager energy of IMF2 is significant as compared to other modes and can be further utilized to detect the HIF.

For accurate and reliable detection of HIF, adaptive threshold selection procedure is included in this work. The adaptive threshold (ζ_{th}) provides support to avoid relay malfunction during switching events, system unbalances, presence of noise and harmonics in the inverter interfaced microgrid system.

In any case, if $\zeta > \zeta_{th}$ then HIF can be detected by the proposed adaptive method. To avoid relay nuisance tripping, one cycle time for observation can be provided to analyze and confirm the occurrence of HIF.

C Adaptive Threshold Setting Process

In this work, an adaptive threshold setting mechanism is provided for secure detection of HIF. The energy estimated using (4) is very high during fault. But the system irregularities cannot be avoided. In order to avoid any unambiguous situations, a standard threshold setting mechanism is included in the proposed method, which is generally adopted in an overcurrent relay. The steps for threshold value selection can be specified as:

Step 1: Extract the local maximum value from one full-cycle data of 'ζ' for every cycle as:

$$\zeta_{i,\max} = \max(\zeta_0, \zeta_1, \ldots\ldots \zeta_{n-1}) \tag{5}$$

where, $i = 0, 1, \ldots\ldots, n\text{-}1$ and n = no. of samples per cycle.

Step 2: Compute threshold setting 'ζ_{th}' using (6):

$$\zeta_{th} = 1.25\zeta_{i,\max} \tag{6}$$

The magnitude of 'ζ_{th}' is dynamic with respect to magnitude changes in 'ζ_B'. To establish a stable reference during normal operation, $\zeta_{i,\max}$ is calculated using (5). For normal operation $\zeta_{i,\max}$ will be small and less than the value generated during fault. $\zeta_{i,\max}$ may deviate significantly from its normal value during the initiations of any transient event. And this change in the value of $\zeta_{i,\max}$ has been considered as a criterion for fault detection. To maintain the dependability feature of the protection function during other switching events, $\zeta_{i,\max}$ is multiplied with 1.25. ζ_{th} in (6) helps the proposed method to maintain a balance between dependability and security. The flow diagram of the proposed method is depicted in Fig. 1.

3. Distribution system architecture and HIF characteristics

D. A. Description of Test System

The performance of proposed algorithm is evaluated on Aalborg model [29] as shown in Fig. 2(a). The original system is modified by substitution of DG-1 & DG-2 with two Type III doubly fed induction generator (DFIG) wind turbines. DG-1 and DG-2 has capacity of 2 MW. DG-3 in the modified system that represents a photovoltaic (PV) unit connected to bus 14. The nominal operating output of PV system is 630 kW. The detailed system parameters are referred from [29]. The modified model is simulated in EMTDC/PSCAD software and for validation of the fault detection algorithm, MATLAB R2016a software is used. The operating and sampling frequencies are 50 Hz and 1 kHz respectively. The operational response of the relay connected to bus-9 is analyzed.

E. B. Characteristics of HIF

The HIF possess two characteristics; one is low fault current and other arcing. The magnitude of fault current is very less or below the load current [30]. The unpredictable and nonlinear nature of the current signal during HIF may vary in the range of zero to less than 100 A [31]. Depending on the system voltage level, the severity of the fault current

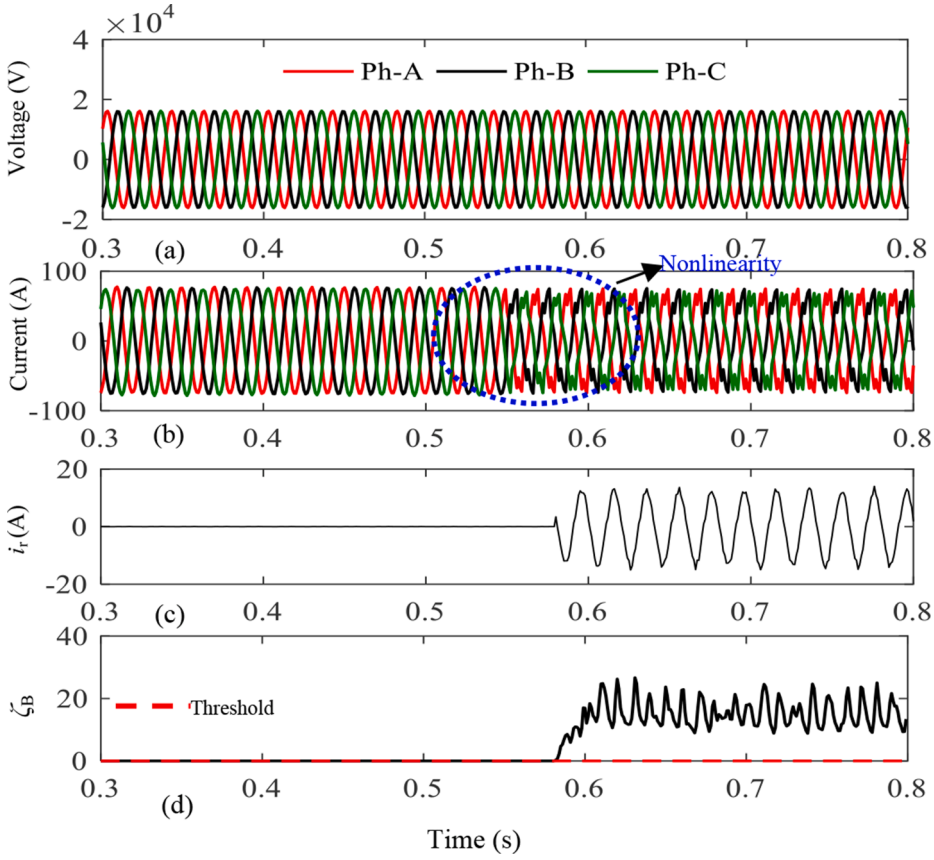

Fig. 12. Response for nonlinear load switching and HIF. Fault time = 0.58 sec, *R*p and *R*n = 800 ~ 1000 Ω.

varies. Due to air gap between the downed conductor and the faulted path, arcing phenomenon gets initiated. The erratic characteristics of the fault current is due to arc extinction and reignition process. The arc current (i) can be expressed as mentioned in (7) mathematically at any instant (n) during acing in terms of the equivalent resistance of the arc (r), arc constant (γ) and the fundamental voltage amplitude of AC component (V_{AC}) during fault.

$$i(n) = \frac{r \quad i(n-1) + \frac{\gamma}{i(n-1)^{1.2}} + 35 - V_{AC}\sin\omega t}{r - \frac{1.2}{i(n-1)^{2.2}}\frac{\gamma}{}} \tag{7}$$

The term r varies, but in practical scenario it does not consistently vary, so a HIF model as shown in Fig. 3 is simulated in EMTDC/PSCAD. There are several HIF models used in the literature [6,12,18]. In this work, the HIF model used in [6] is used. V_p and V_n are the two DC sources, D_p and D_n are the corresponding diodes. The value of arc resistance (r) in (7) is similar to the value of R_p and R_n. v_{ph} is analogous to V_{AC} i.e. the instantaneous voltage. V_p and V_n can be adjusted to vary the arc suppression time during the nonlinear fault. The conduction of current to the ground is possible only when $v_{ph} > V_p$ and in the reverse direction for $v_{ph} < V_n$. There will be no current flow, when v_{ph} lies between V_p and V_n. R_p and R_n are varied in the range of 10 ~ 1500 O for different simulated cases to analyze the performance of proposed approach. v_{ph} depends on radial distribution system model taken in the study. The v-i characteristics of the HIF model is shown in Fig. 4.

4. Performance analysis

To check the performance of the MCEEMDAN technique as proposed in this paper in terms of speed, adaptability, reliability, dependability and security, the test system (Fig. 2) is simulated. The value of ζ_B is monitored continuously for detection of HIF. The speed of proposed adaptive method is verified by monitoring the detection time for individual fault cases. For adaptability analysis, system operating conditions and architecture have been considered. Reliability and security aspects of protection functions are analyzed by varying the fault scenario such as fault inception time, fault location, and fault resistance. Relay security is also tested for distorted signal i.e., signal contaminated with white Gaussian noise (WGN), presence of harmonics, sag and unbalances.

F. A. Fault with Voltage Sag, Noise, Harmonics and Unbalances

The impact of presence of noise, harmonics, voltage sag and unbalance loading in the individual phases, on the performance of proposed technique is evaluated. The HIF model parameters are set as: *V*p and *V*n in the range 100 ~ 1000 V and *R*p and *R*n in the range 40 ~ 150 Ω. The WGN of signal to noise ratio (SNR) 5 dB is considered. Phase-A loading is increased to 10%. 3rd-harmonic component is added to the current signal. The fault in phase-A at 0.5 sec is created, which causes sag in the corresponding phase voltage as observed in Fig. 5 (a). The distorted three-phase currents are shown in Fig. 5 (b). After fault inception, a small variation in the faulty phase current can be noticed. Also, the residual current as shown in Fig. 5 (c) is nonzero before occurrence of the fault and unsymmetrical after the fault. An estimation error can be expected in the phasor component which may deteriorate fault analysis. But using time–frequency analysis, the fault signal in time domain can be analyzed. Using (4), energy index is generated and compared to the adaptive threshold for event identification. From Fig. 5 (d), ζ_B lies above ζ_{th} after the onset of fault and this triggers the decision of the relay once applied using the proposed algorithm. The given index exceeds selected threshold just after 1 ms of the fault initiation, but as HIF often continues for many cycles, one cycle time period can be considered to check the continuity of the fault. The breaker operation time can also be set accordingly. It is to be noted that during intermittent fault using the

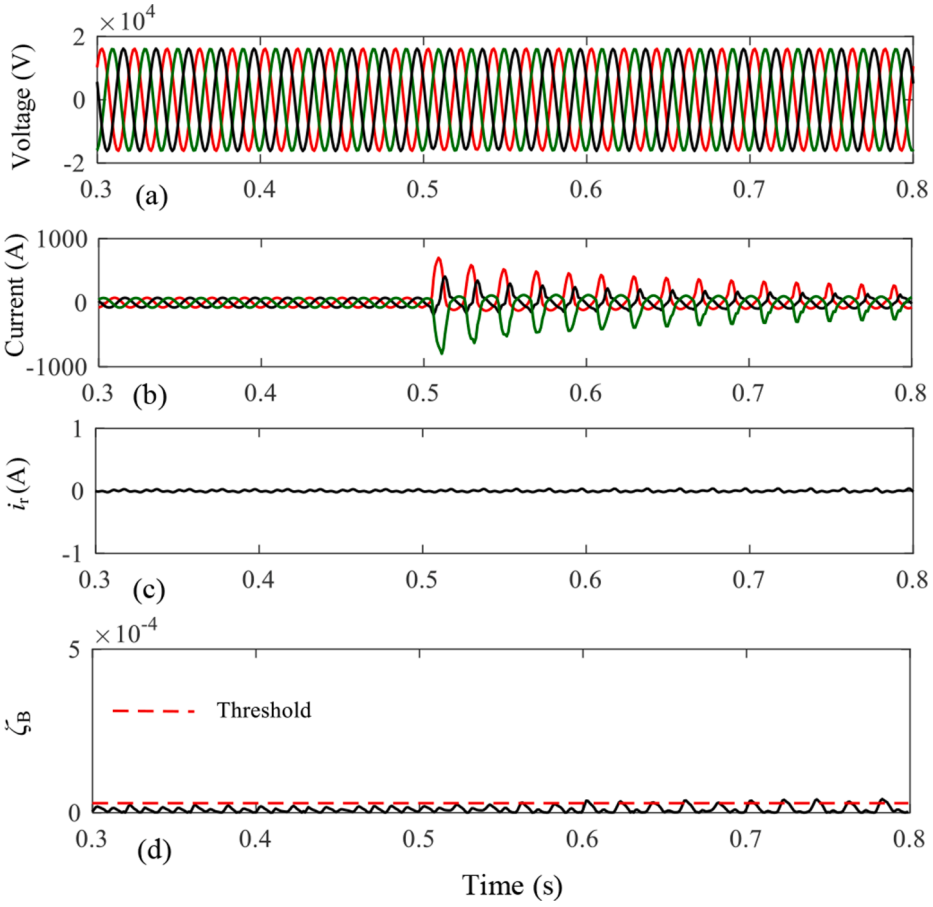

Fig. 13. Response for Transformer Switching/Energization.

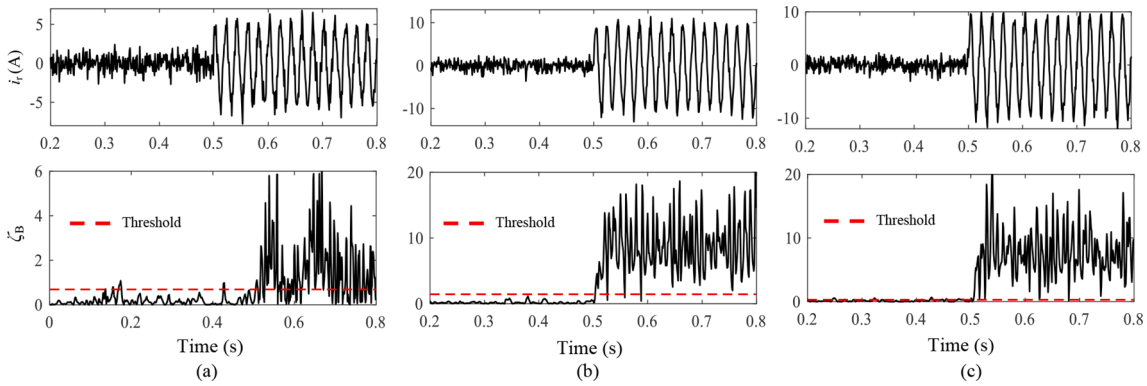

Fig. 14. Response for different ground configurations. (a) Ungrounded system, (b) High resistance grounding, (c) Resonant grounding. SNR = 5 dB, fault between bus 7–8, *R*p and *R*n = 1 ~ 1.15 kΩ.

proposed method, detection time can be low and tripping decision can be taken accordingly.

To test the speed of operation as well as security and reliability of the method, SNR is varied from 5 to 35 dB along with loading level and harmonic content in the current signal. The details of test cases are articulated in Table 1. The faults are created at 0.5 sec in phase-A. The values of *V*p and *V*n in the range 100 ~ 1000 V and *R*p and *R*n in the range 40 ~ 150 Ω have been considered. The results for different simulated cases are shown in Fig. 6. The adaptive threshold for individual cases computed using (5) and (6) remain reliable to detect the fault. Due to the presence of noise, harmonics and unbalance loading, the current signal remains highly distorted. The noise immunity capacity of MCEEMDAN approach helps in extracting the suitable noise-free mode for development of reliable and secured detection index. Also, the response of the method is fast as the index rises above the threshold just after the inception of the fault. The adaptive threshold acts as a low pass filter which supports the MCEEMDAN technique in decision making. The results for all the simulated cases as mentioned in Table 1 and illustrated in Fig. 6 proves the efficacy of proposed fault detection algorithm.

G. B. Modes of Operation

During islanded mode of operation, the current contribution by DG

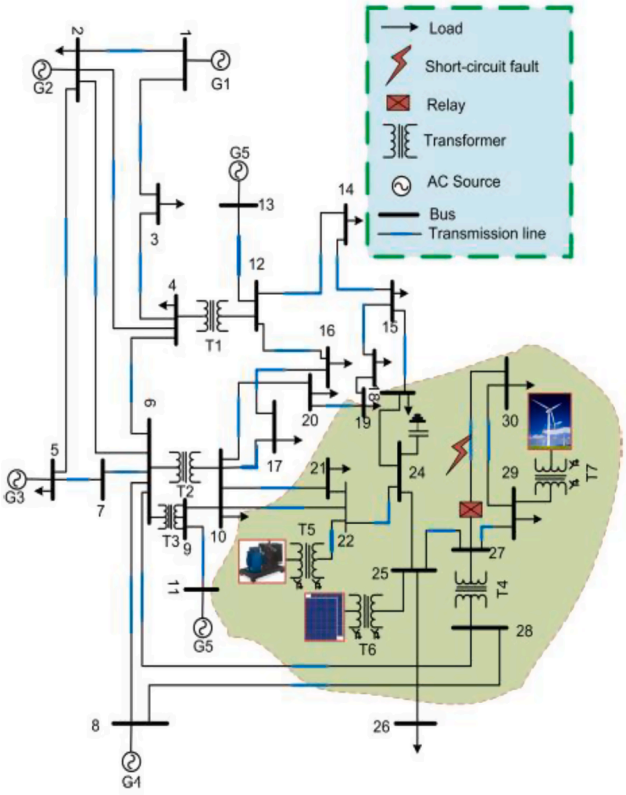

Fig. 15. Modified IEEE 30 bus system with distributed energy resources.

to the fault point is very small and hence detection of fault under such condition is challenging. To evaluate the performance of the method during islanded mode, the PCC circuit breaker (CB) is kept open and a HIF is created at 0.5 sec in the line between bus 9–10. The values of *R*p and *R*n are considered in the range of 1 ~ 1.35 kΩ. The WGN of 10 dB is added to the current signal. The current and voltage waveforms for this simulated case are illustrated in Fig. 7. As can be observed in Fig. 7 (b), the current signature does not change significantly and it is difficult to identify as a fault by conventional overcurrent relay. Residual current is also highly distorted and nonzero as can be observed in Fig. 7 (c). The energy index in Fig. 7 (d) is more than threshold and this is sufficient to detect the HIF. The index exceeds the threshold just after the inception of the fault. So, quick detection of HIF under islanded mode of operation is possible using adaptive MCEEMDAN based approach.

H. C. Change in Fault Location, Fault Resistance, and Inception Time

The distribution network (Fig. 2) is simulated for other fault cases by varying the fault location on the line, fault resistance and inception time. The impact of fault location, resistance and inception time is significant to indicate the reliable and secure operation of detection algorithm. All these cases are simulated under islanded mode of operation of the distribution system. The effectiveness of adaptive MCEEMDAN technique is illustrated for faults at 75%, 85% and 95% on line from the relay location in Fig. 8. With increasing fault distance from relay position, the effectiveness on the measured signal reduces. This creates problem in detecting HIF. In the test system, relay is connected near bus-9 and faults are created in the line between buses 9–10. In Fig. 8, three different cases for 75%, 85% and 95% fault locations are presented. While varying the fault location, *R*p and *R*n in the range 1.35 ~ 1.5 kΩ have been considered with SNR of 10 dB. Faults resistances are also varied for *R*p and *R*n in the range 500 ~ 2 kΩ and results are shown in Fig. 9. It is clearly indicated that fault is accurately detected. Next in study, fault at voltage peak, zero crossing and other points on voltage wave have been created and obtained results are shown in Fig. 10. In all the simulated results detection time is the same as discussed above. The adaptive threshold is suitable enough to detect HIF accurately irrespective of fault and system operating conditions. Thus, speed of HIF detection, accuracy, security, and reliability aspects can be maintained using the proposed method. It is also observed from the results that detection time does not vary with the change in system and fault conditions.

I. D. Capacitor Charging (CC)

The selectivity feature of protective algorithm should be capable of differentiating non-fault events against fault events. The charging or switching ON and OFF condition of capacitor bank connected to any distribution system generates high frequency components in the voltage and current signal. So, it is quite natural that methods operated on the basis of even and odd harmonics can get affected. Thus, it is essential to evaluate such condition in order to check the dependability feature of the proposed approach.

Both CC and HIF cases are created at different instances. First, a three-phase, 1.5 MVAr capacitor bank connected near bus 10 is switched ON at 0.5 s following which, after 3 cycles i.e., at 0.56 s, a fault is created on phase-C. For the fault, *R*p and *R*n are considered in the range of 800 ~ 1000 Ω. The transients in voltage and current signals can be observed from Fig. 11 (a) and (b). The residual current and detection index (ζ_B) are shown in Fig. 11 (c) and (d) respectively. The index exceeds the threshold just after inception of fault but remains below the threshold at the instant of charging of capacitor bank. The proposed method uses the current signal for HIF detection. The CC also introduces significant transients at the instant of switching but the energy generated during HIF for the physical change in system condition is more as compared to CC and thus it remains below the threshold. Adaptive threshold can enhance the operation of HIF detection logic during such dependable cases, and thus ensures the secure operation of relay.

J. E. Nonlinear Load Switching (NLS)

The performance of proposed approach is also evaluated for NLS, followed by a HIF occurrence. For this, a three-phase diode rectifier with resistive load of 0.5 MW is used. The load is connected at bus 10 of the microgrid test system (Fig. 2). The load is switched ON at 0.55 sec, while fault is created on phase-B at 0.58 sec. The fault resistance varies in between 800 ~ 1000 Ω. The voltage and current waveforms, calculated residual current and energy index are shown in Fig. 12. After switching of nonlinear load at bus 10, current signal gets highly distorted as seen from Fig. 12 (a). The decomposition capability of MCEEMDAN is reliable and the energy index with adaptive threshold helps to identify only HIF, which can be observed in Fig. 12(d). So, the method is dependable during NLS as evident from the obtained results.

K. F. Transformer Switching (TS)

To conduct the dependability analysis, transformer energization condition is simulated. Transformer energization in distribution system often possess challenges to many protection algorithms due to the presence of even harmonics such as 2nd and 4th along with decaying DC. The inrush phenomenon lasts for more than 15 to 20 cycles. These components are also the key components using which detection task of HIF is conducted. The transformer connected to CHP bus (Fig. 2) is energized at 0.5 s. The three phase voltages and currents along with proposed index are depicted in Fig. 13. Adaptive threshold is computed using (5) and (6). The three phase voltage and current waveforms are shown in Fig. 13 (a) and (b) respectively. The energization event introduces inrush phenomenon during core saturation as observed in Fig. 13 (b). Using residual current (Fig. 13 (c)), the proposed index is computed and compared to the threshold. Unbalance in phases can be extracted from the output of residual current. The use of MCEEMDAN

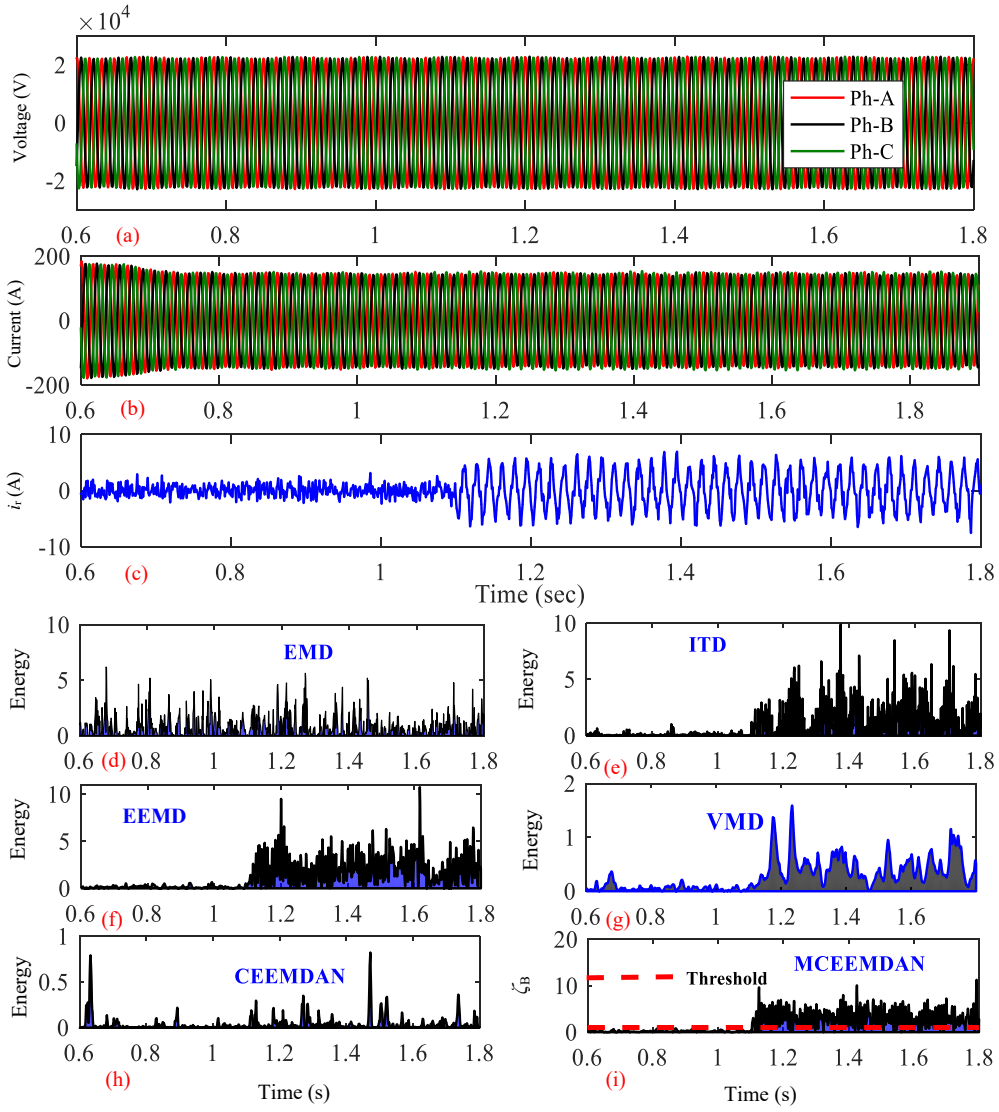

Fig. 16. Comparative analysis for HIF on modified IEEE 30 bus radial network. SNR = 5 dB, fault between bus 27–30, *R*p and *R*n = 3 ~ 3.5 kΩ.

helps in signal decomposition but as the change in physical energy for IMF2 is not significant, the proposed index remains very small. So, from Fig. 13 (d), it can be confronted that the method is immune to TS and also for the tested switching cases, it is dependable.

L. G. System Grounding

The distribution network transformers can have different configurations in terms of connection of three phase windings. In order to limit the amount of ground fault current in distribution system, ungrounded, high resistance, and resonant grounding configurations are adopted [32,33]. Due to low contact path, any fault occurrence during the fault period may not be detected properly. Thus, to study the impact of grounding on fault detection criteria, different configurations are considered in study and the response of adaptive threshold based MCEEMDAN technique is discussed. The main applications of high impedance grounding system are in generator-transformer connected system and medium voltage distribution system connected to industrial power plants. In resonant grounding, high impedance reactor used to neutralize the system phase-to-ground capacitance is to be connected at ground path. The ground-fault or variable impedance neutral reactor is a Peterson coil or arc suppression coil. The configuration of the transformer connected to PCC bus in the test system is set according to ground connections; ungrounded, high resistance and resonant grounding. The HIF on line between bus 7–8 is created. The fault resistance value is varied in the range 1 ~ 1.15 kΩ. Fig. 14 (a) shows the results for ungrounded configuration, while Fig. 14 (b) and (c) for high resistance and resonant grounding respectively. The residual current measured at bus 7 is shown in upper subplot, while the index value is plotted in lower subplot. In all the three cases, SNR 5 dB is added to the current signals. Fault inception time is 0.5 sec. After the fault, the neutral current varies and it is highly distorted. But the response of MCEEMDAN based HIF detection is hardly affected by the grounding configuration.

M. H. Comparison with other Available Advanced Methods

For further analysis and to validate the adaptability of proposed MCEEMDAN based HIF detection technique, a large power network is considered next. The IEEE 30 bus radial network [34] shown in Fig. 15 is simulated. However, the network is modified by including a diesel generator, wind turbine and PV system at bus 22, 29 and 25 respectively. The capacity of wind turbine, PV and diesel generator system is 6 MW, 3 MW and 1 MW respectively. The HIF is created on the line between bus 27–30 and continues up to 1.9 sec. Relay is connected at bus 27. The nominal frequency of system is 60 Hz and data is acquired every 1 ms. The already reported time–frequency techniques such as EMD [35],

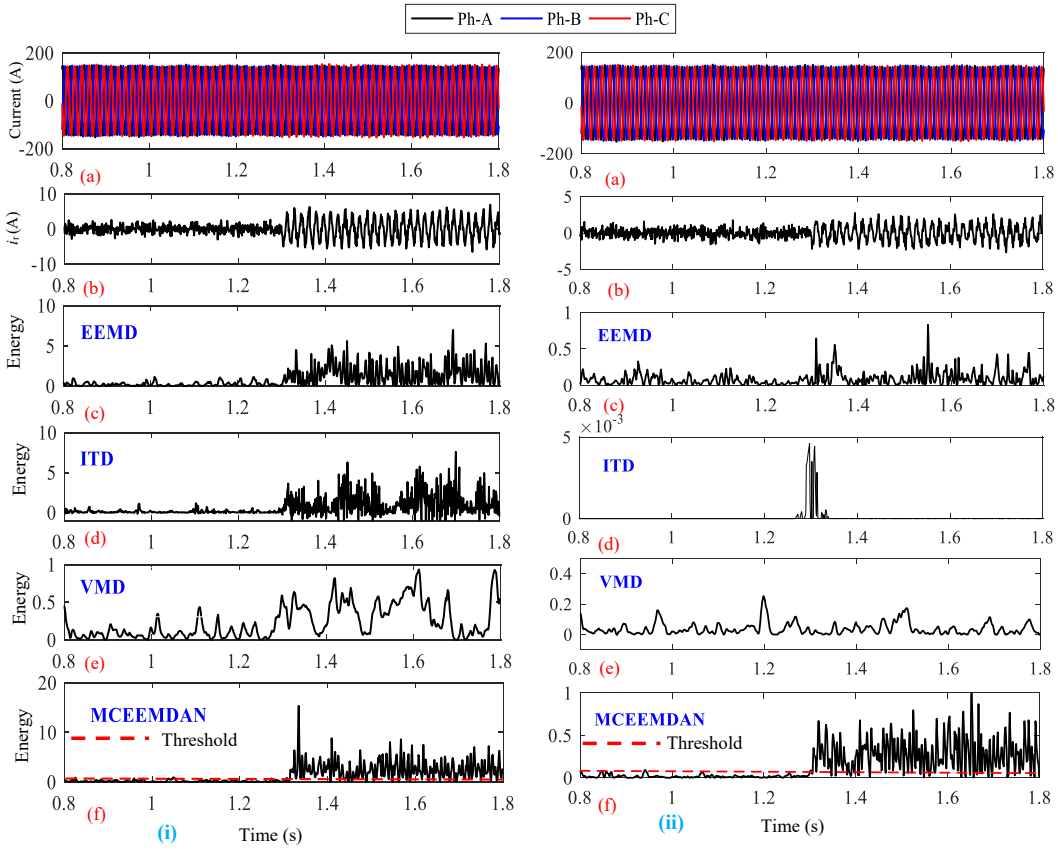

Fig. 17. Comparative analysis for HIF on modified IEEE 30 bus radial network. (i) HIF = 10 ~ 11 kΩ, WGN = 10 dB, (ii) HIF = 3 ~ 11 kΩ, WGN = 5 dB.

EEMD [36], VMD [18], ITD [20], and CEEMDAN [22] are also considered for comparative analysis with proposed approach. The HIF in the range of 3 ~ 3.5 kΩ is created on the line 30–27 and the fault current signal is superimposed with 5 dB SNR. The three phase voltage and current waveforms can be observed from Fig. 16 (a) and (b) respectively. Considering the individual phase information, residual current is computed as shown in Fig. 16 (c) and the same is decomposed using EMD, EEMD, ITD, VMD, CEEMDAN and MCEEMDAN techniques. The decomposed IMF2 using these techniques are used to estimate the energy. The performance of respective techniques are shown in Fig. 16(d)-(i). The EMD, and CEEMDAN techniques are biased due to the presence of noise. The variation in energy plots for these two techniques cannot be identified before and after fault event. Due to the presence of noise, non-fault situations cannot be discriminated against HIF event. On other hand, the performances of EEMD, ITD, VMD and MCEEMDAN techniques are proved to be better, secured and reliable.

To further analyze the sensitivity and dependability of EEMD, ITD, VMD and MCEEMDAN techniques, two different HIFs under different circumstances are created. In the first case, to analyze the sensitivity of all the methods, an HIF with a fault resistance in the range of 10 ~ 11 kΩ and signal contaminated with 10 dB WGN is created on the line 30–27 of the modified IEEE 30 bus test system. Next, for ungrounded configuration of all the transformers connected to bus-27 in the modified IEEE 30 bus test system and an HIF of 3 ~ 3.5 kΩ and signal contaminated with 5 dB WGN is created on the line 30–27. Fault inception time for both the cases are 1.3 s.

The three-phase current generated during fault case, residual current, response of EEMD, ITD, VMD and MCEEMDAN technique is shown in Fig. 17 (i) and (ii) respectively. The results for the first fault case (HIF with 10 ~ 11 kΩ) are shown in Fig. 17 (i) and the results for HIF in an ungrounded system are shown in Fig. 17 (ii). The three phase currents for both the fault cases are shown in Fig. 17 (i)(a) and (ii) (a) respectively. Due to the nature of the fault path and absence of ground path, current variation after the occurrence of fault at 1.3 s is negligible. Presence of noise in the current signal, create distortions in the residual currents (Fig. 17 (i)(b) and (ii)(b)). But the deviations in residual current is very less in ungrounded fault case as compared to other HIF case. The sensitivity of EEMD technique may degrade with the increase in fault path resistance (Fig. 17(i) (c)) and can affect the relay security in an ungrounded system. Similarly, the response of ITD technique is unreliable in an ungrounded system. VMD technique is not suitable for very HIF case and also for ungrounded system. Even for very HIF and in an ungrounded system, the proposed MCEEMDAN technique is reliable with the help of set adaptive threshold value. Also, the sensitivity and security of the MCEEMDAN technique is independent of network configuration.

5. Conclusion

This paper presented an adaptive HIF detection approach for renewable penetrated distribution network using modified CEEMDAN technique. The residual current signal from local measurements was decomposed using MCEEMDAN technique and subsequently, the energy of high frequency content, i.e IMF2 was calculated. The computed energy was then compared against the adaptive threshold value. As an efficient filter, MCEEMDAN delivers noise free signal and thus presence of noise content in the signal was not at all an issue in the detection process. The non-fault events; CS and NLS cannot bias the performance of proposed approach. Though, the level of fault current varies obviously during grid connected and islanded mode, but the impact on reliable detection using proposed approach was negligible. In order achieve developed protection function, suitable in practical domain, short window data signal was passed to process through MCEEMDAN technique. Based on the simulation studies conducted in the paper, it was

demonstrated that the performance of proposed approach remains consistence in reliable detection of HIF, even in presence of noise, harmonics, unbalance loading, grounding configuration, fault location, fault time and fault resistance. This was due to the fact that adaptive threshold helps to discriminate the fault events against non-fault events correctly. The method is dependable against the tested switching events such as capacitor charging, nonlinear load switching and transformer energization. The impact of grid operating modes on the detection performance remained negligible and at the same time, the speed of HIF detection and accuracy was high.

CRediT authorship contribution statement

Monalisa Biswal: Conceptualization, Data curation, Formal analysis, Supervision, Writing – original draft, Writing – review & editing. **Ch. Durga Prasad:** Methodology, Validation, Writing – review & editing. **Papia Ray:** Validation, Visualization, Writing – original draft. **Nand Kishor:** Formal analysis, Supervision, Writing – review & editing.

Declaration of Competing Interest

The authors declare that they have no known competing financial interests or personal relationships that could have appeared to influence the work reported in this paper.

References

[1] Report of IEEE PSRC Working Group D15, High impedance fault detection technology. 1996. [Online]. Available: http://grouper.ieee.org/groups/td/dist/documents/highz.pdf.

[2] Aucoin BM, Jones RH. High impedance fault implementation issues. IEEE Trans Power Del Jan. 1996;11(1):139–48.

[3] Reason J. Relay detects down wires by fault current harmonics. Electric World Dec. 1994;208(12):58–9.

[4] Girgis AA, Chang W, Makram EB. Analysis of high-impedance fault generated signals using a Kalman filtering approach. IEEE Trans Power Del Jan. 1990;5(4):1714–24.

[5] Sarlak M, Shahrtash SM. High impedance fault detection using combination of multi-layer perceptron neural networks based on multiresolution morphological gradient features of current waveform. IET Gener Transm Distrib May 2011;5(5):588–95.

[6] Gautam S, Brahma SM. Detection of high impedance fault in power distribution systems using mathematical morphology. IEEE Trans Power Syst May 2013;28(2):1226–34.

[7] Cui T, Dong X, Bo Z, Juszczyk A. Hilbert-transform-based transient/ intermittent earth fault detection in noneffectively grounded distribution systems. IEEE Trans Power Del Jan. 2011;26(1):143–51.

[8] Li Y, Meng X, Song X. Application of signal processing and analysis in detecting single line-to-ground (SLG) fault location in high impedance grounded distribution network. IET Gener Transm Distrib Feb. 2016;10(2):382–9.

[9] Soheili A, Sadeh J, Bakhshi R. Modified FFT based high impedance fault detection technique considering distribution non-linear loads: Simulation and experimental data analysis. Int J Elect Power Energy Syst Jan. 2018;94:124–40.

[10] Wang B, Geng J, Dong X. High-impedance fault detection based on nonlinear voltage–current characteristic profile identification. IEEE Trans Smart Grid Jul. 2018;9(4):3783–91.

[11] Moravej Z, Mortazavi SH, Shahrtash SM. DT-CWT based event feature extraction for high impedance faults detection in distribution system. Int Trans Elect Energy Syst Dec 2015;25(12):3288–303.

[12] Costa FB, Souza BA, Brito NSD, Silva JACB, Santos WC. Real-time detection of transients induced by high impedance faults based on the boundary wavelet transform. IEEE Trans Ind Appl 2015;51(6):5312–23.

[13] Yi Z, Etemadi AH. Fault detection for photovoltaic systems based on multi-resolution signal decomposition and fuzzy inference systems. IEEE Trans Smart Grid May 2017;8(3):1274–83.

[14] Lien K-Y, et al. Energy variance criterion and threshold tuning scheme for high impedance fault detection. IEEE Trans Power Del Jul. 1999;14(3):810–7.

[15] Mamishev AV, Russell BD, Benner CL. Analysis of high impedance faults using fractal techniques. IEEE Trans Power Syst Feb. 1996;11(1):435–40.

[16] Sheng Y, Rovnyak SM. Decision tree-based methodology for high impedance fault detection. IEEE Trans Power Del Apr. 2004;19(2):533–6.

[17] Kar S, Samantaray SR. Time-frequency transform-based differential scheme for microgrid protection. IET Gener Transm Distrib Feb. 2014;8(2):310–20.

[18] Wang X, Gao J, Wei X, Song G, Wu L, Liu J, et al. High impedance fault detection method based on variational mode decomposition and Teager-Kaiser energy operators for distribution network. IEEE Trans Smart Grid 2019;10(6):6041–54.

[19] Aucoin B, Russell B. Distribution high impedance fault detection utilizing high frequency current components. IEEE Trans. Power App. Syst. Jun. 1982;PAS-101(6):1596–606.

[20] Biswal M., Ghore S., Malik O.P., Bansal R.C. "Development of time-frequency based approach to detect high impedance fault in an inverter interfaced distribution system", *IEEE Transactions on Power Delivery*, 2021, Early Access, DOI: 10.1109/TPWRD.2021.3049572.

[21] Lima EM, Coelho RDA, Brito NSD, Souza BAD. High impedance fault detection method for distribution networks under non-linear conditions. Int J Elect Power Energy Syst Oct. 2021;131:107041. https://doi.org/10.1016/j.ijepes.2021.107041.

[22] Colominas MA, Sclotthauer G, Torres ME. Improved complete ensemble EMD: A suitable tool for biomedical signal processing. Biomedical Signal Processing and Control Nov. 2014;14(1):19–29.

[23] Ding F, Li X, Qu J. Fault diagnosis of rolling bearing based on improved CEEMDAN and distance evaluation technique. J Vibroeng 2017;19(1):260–75.

[24] Xiaoli L, Chengwei L. Improved CEEMDAN and PSO-SVR modeling for near-infrared noninvasive glucose detection. Comput Math Methods Med 2016.

[25] Yu DC, Khan SH. An adaptive high and low impedance fault detection method. IEEE Trans on Power Del Oct. 1994;9(4):1812–21.

[26] Jwon WH, Lee GW, Park YM, Yoon MC, Yoo MH. High impedance fault detection utilizing incremental variance of normalized even order harmonic power. IEEE Trans on Power Del Apr. 1991;6(2):557–64.

[27] Wu Z, Huang NE. Ensemble empirical mode decomposition: A noise-assisted data analysis method. Adv Adapt Data Anal Jan. 2009;1(1):1–41.

[28] Torres ME, Colominas MA, Schlotthauer G, Flandrin P. A complete ensemble empirical mode decomposition with adaptive noise. In: in 2011 IEEE International Conference on Acoustics, Speech and Signal Processing (ICASSP), May; 2011. p. 4144–7.

[29] Nale R, Biswal M, Kishor N. A transient component-based approach for islanding detection in distributed generation. IEEE Trans on Sustain Energy July 2019;10(3):1129–38.

[30] Li J, Kohler JL. New insight into the detection of high-impedance arcing faults on DC trolley systems. IEEE Trans Ind Appl 1999;35(5):1169–73.

[31] Hou D. Detection of high-impedance faults in power distribution systems, 6th Annual Clemson University Power System Conference, Clemson, South Carolina, march 13-16, 2007.

[32] Roberts J., Altuve H.J., Hou D. Review of ground fault protection methods for grounded, ungrounded, and compensated distribution systems. Online: https://selinc.com/api/download/2604.

[33] C62.92.1-2016-IEEE, "Guide for the application of neutral grounding in Electrical utility systems-part-1 Introduction," DOI: https://doi.org/10.1109/IEEESTD.2017.7891430, March 2017.

[34] Christie R. Power System Test Archive, Aug. 1999. [Online]. Available: http://www.ee.washington.edu/reserach/pstca.

[35] Biswal S, Biswal M. Fault-swing discrimination using Hilbert-Huang transform integrated discrete teager energy operator. IET Sci Meas Technol October 2018;12(7):829–37.

[36] Xue S., Cheng X., Lv X. High resistance fault location of distributed network based on EEMD, *In Proceedings of the 9th International Conference on Intelligent Human-Machine Systems and Cybernetics*, Hangzhou, China, 26-27 August 2017; Vo. 1, pp. 322-326.